Supplementary Figure S1

S1A

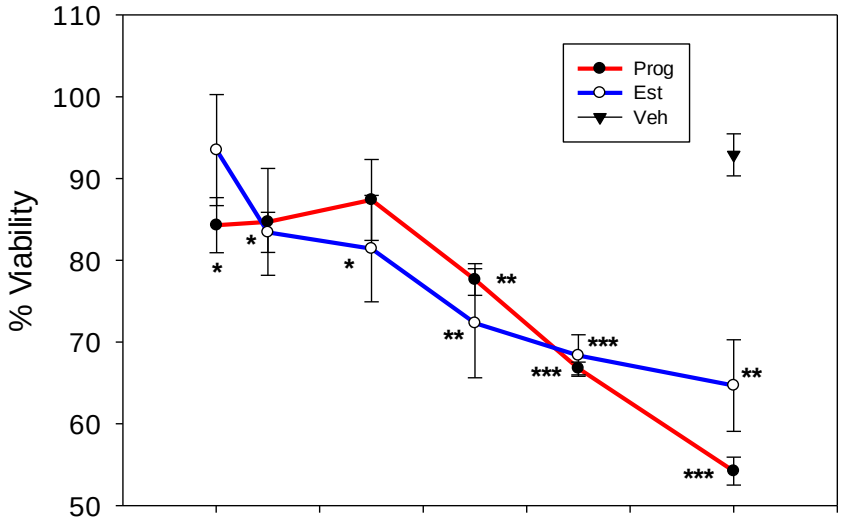

S1B

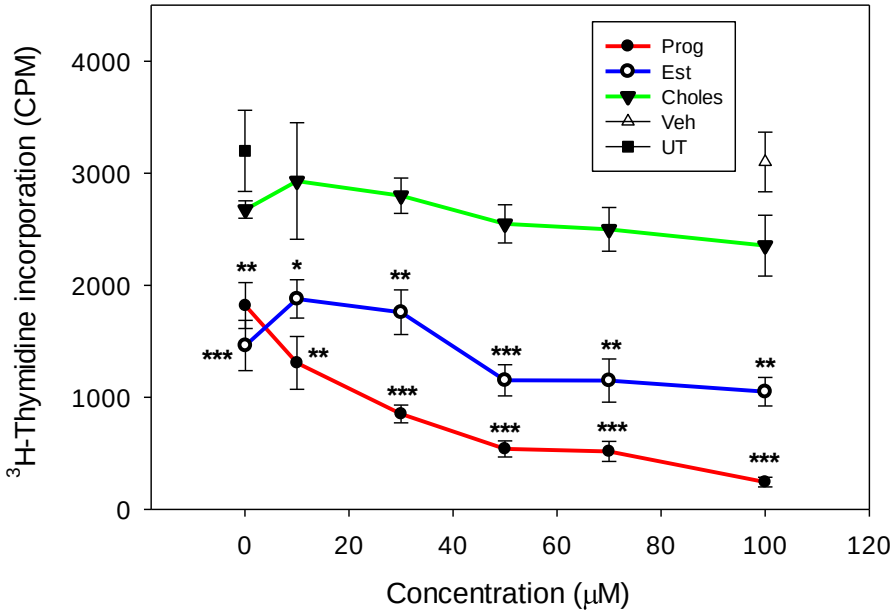

Fig. S1. Ovarian hormones exhibit growth inhibitory effects on A549 cells. (A) A549 cells were incubated with varying concentrations (0.1-100 μM) of Progesterone (Prog) or Estradiol (Est) for 48 h. Cell viability was assessed by MTT. Data is plotted as % viability over untreated cells. Values represent mean ± SD (n=3). Values were compared with highest concentration of the vehicle (Veh). *p<0.05, **p<0.01, ***p<0.001 by the Unpaired t-test. (B) Experimental-set up identical to Figure S1A. Proliferation was assessed by measuring the incorporation of ^{3}H-thymidine. Values represent arithmetic mean ± SD (n=3). Values were compared with corresponding values of negative control; cholesterol (Choles). *p<0.05, **p<0.01, ***p<0.001 by the Unpaired t-test. UT: Untreated cells.

Supplementary Figure S2

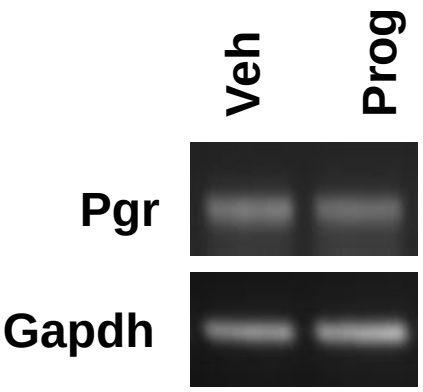

Fig. S2. Progesterone does not induce the expression of its nuclear receptors on LLC1 tumor cells. LLC1 tumor cells were incubated with 50 μM Prog or Veh for 24 h. 1 μg of total RNA was reverse transcribed to cDNA, and PCR carried out for progesterone nuclear receptors (Pgr). Gapdh for the same experiment is shown. The primer used for Pgr (sequence provided in TABLE S2) can amplify both isoforms (A and B) of this receptor. Mirror images of the original gel lanes are shown (raw data provided).

Supplementary Figure S3

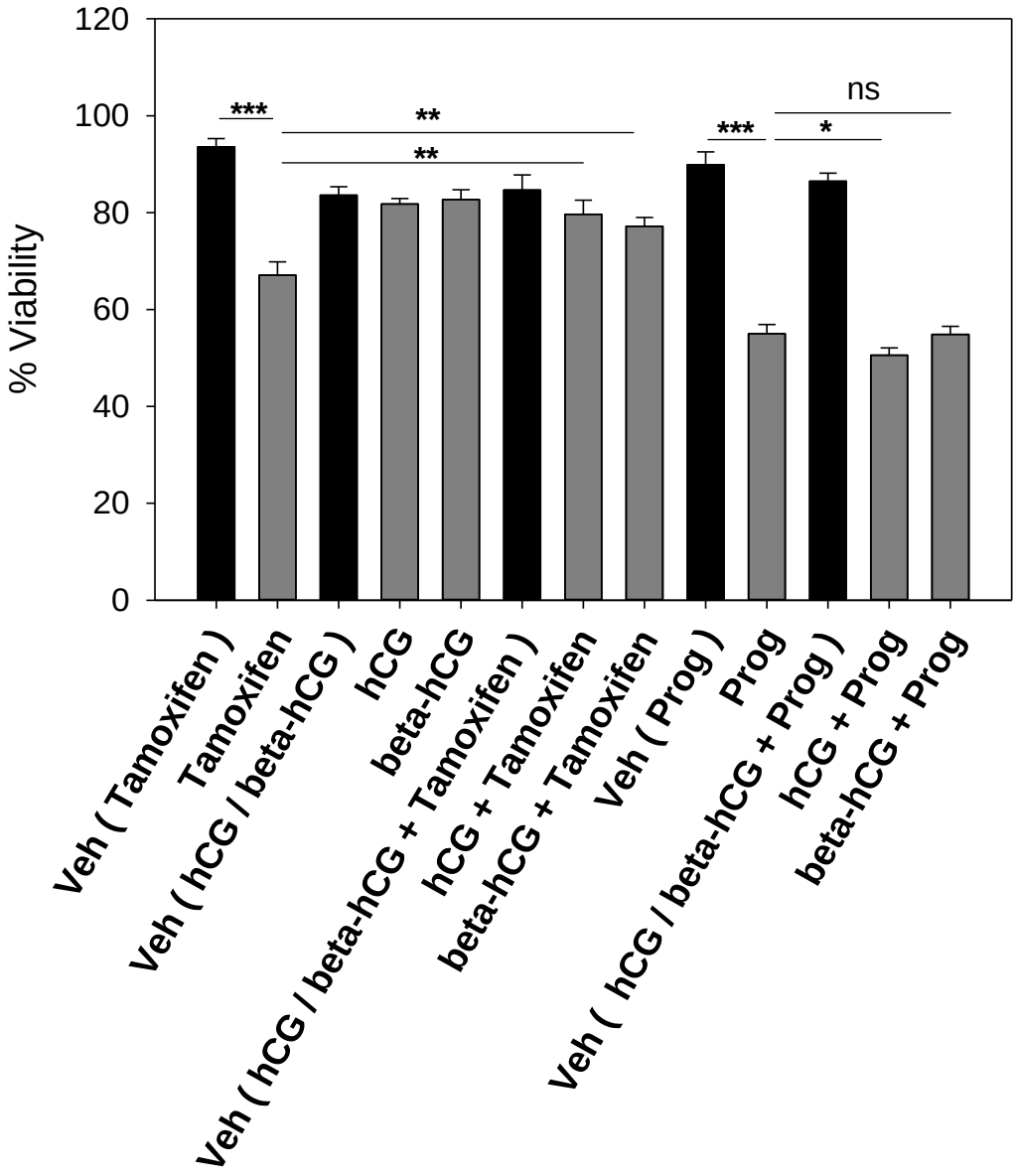

Fig. S3. hCG/beta-hCG can protect LLC1 tumor cells from drug-induced death but not from progesterone-induced death. LLC1 tumor cells pre-incubated with hCG / beta-hCG (0.026 μM) for 24 h followed by treatment with either Tamoxifen (10 μM) or Prog (50 μM) for an additional 24 h. Veh (Tamoxifen) = DMSO; Veh (hCG / beta-hCG) = PBS; Veh (hCG / beta-hCG+Tamoxifen) = PBS+DMSO; Veh (hCG / beta-hCG+Prog) = PBS+ethanol. Cell viability was assessed by MTT. Data is plotted as % viability over untreated cells. Values represent arithmetic mean ± SD (n=3). *p<0.05, **p<0.01, ***p<0.001 by the Unpaired t-test. ns: non-significant.

Supplementary Figure S4

S4A

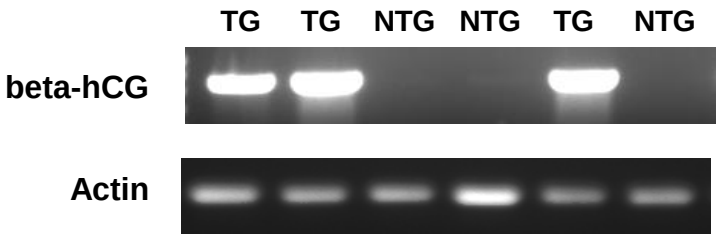

S4B

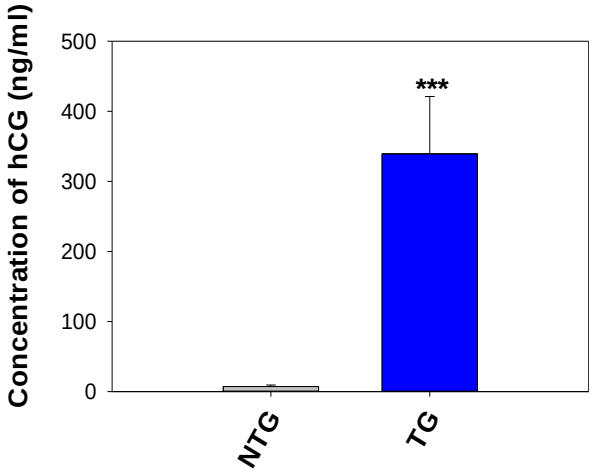

S4C

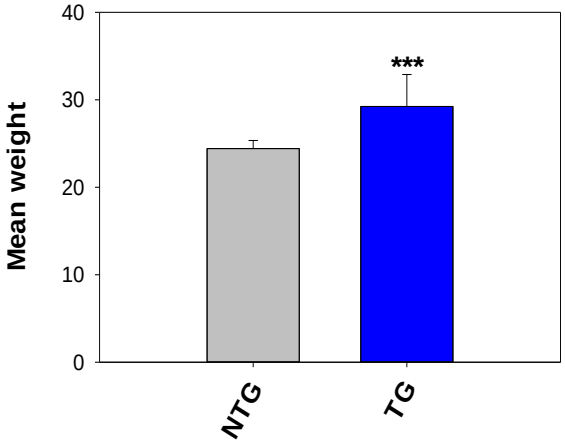

S4D

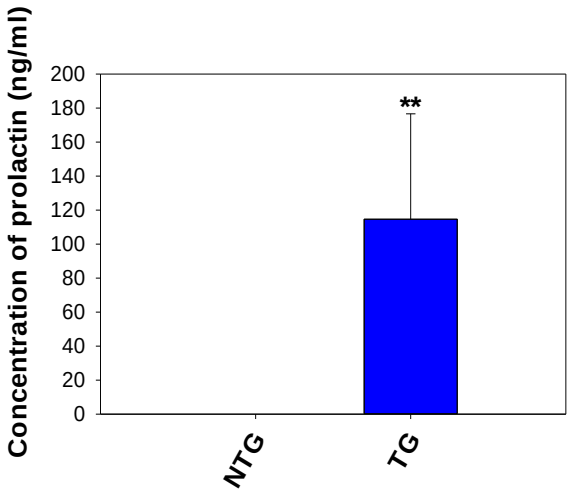

S4E

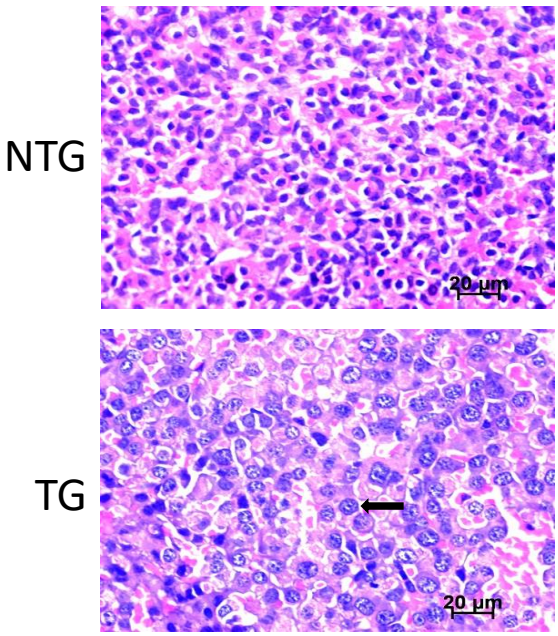

S4F

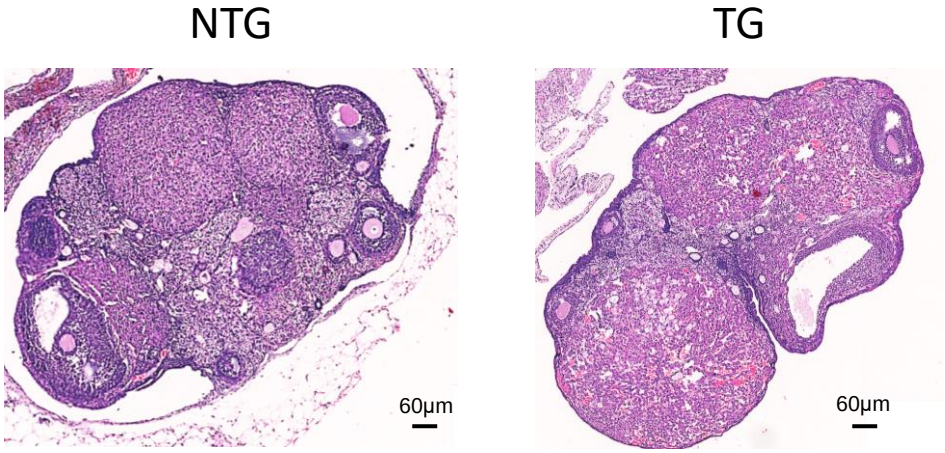

Fig. S4. Identification and characterization of beta-hCG transgenic mice. (A) PCR on genomic DNA from tail clips for detection of the beta-hCG transgene. (B) Radioimmunoassay on serum for the detection of beta-hCG in serum, (n=21). (C) Body weight analysis (at 5 months), (n=21). (D) Prolactin levels (at 17 months), (n=5). (E) Hematoxylin/Eosin staining of histological sections of pituitaries (at 18 months). Arrow indicating adenomas in TG. (F) Hematoxylin/Eosin staining displaying gross histology of ovaries (at 18 months).

All Values represent arithmetic mean ± SD. **p<0.01, ***p<0.001 by the Unpaired t-test. NTG: Non-Transgenic; TG: Transgenic.

Supplementary Figure S5

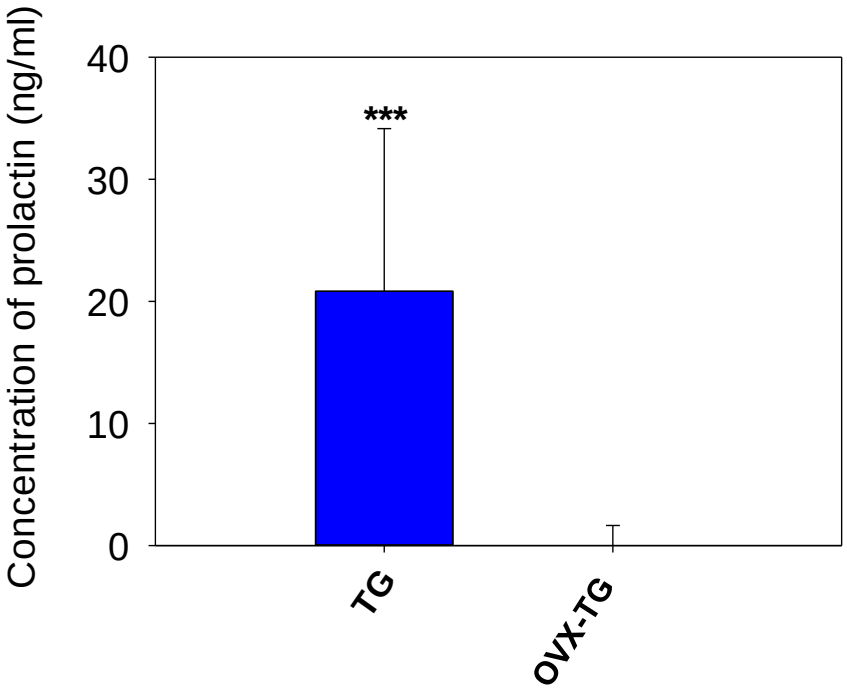

Fig. S5. Ovariectomy in beta-hCG transgenic mice diminishes serum prolactin levels. Serum prolactin levels of 5-6 months old TG and ovariectomized TG (OVX-TG) mice. Values represent arithmetic mean ± SD, (n=23). ***p<0.001 by the Unpaired t-test.

Supplementary Figure S6

S6A **S6B**

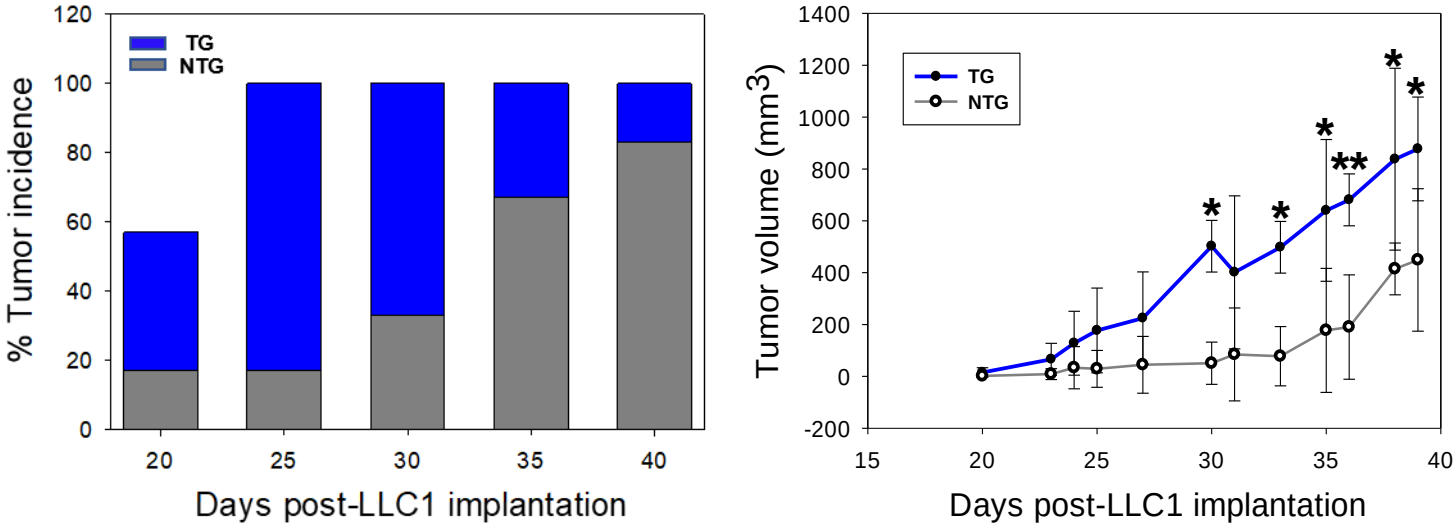

Fig. S6. Enhanced LLC1 tumor incidence and volumes in TG mice. LLC1 tumor cells were implanted into 8-month-old NTG and TG mice. (A) Tumor incidences, (n=8). (B) Tumor volumes. Values represent arithmetic mean ± SD, (n=6). *p<0.05, **p<0.01 vs NTG by Two-way ANOVA, followed by the Bonferroni multiple comparison test.

Supplementary Figure S7

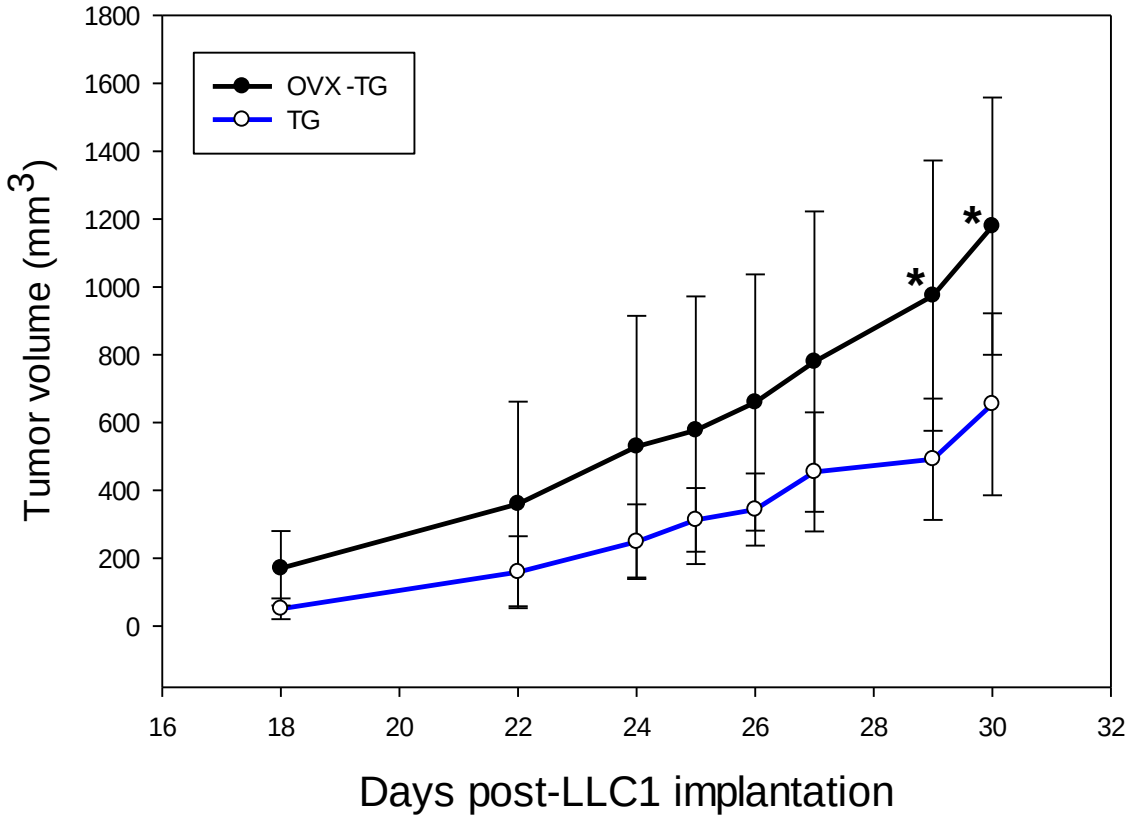

Fig. S7. Enhanced LLC1 tumor growth in beta-hCG transgenic mice upon ovariectomy. Values represent arithmetic mean ± SD, (n=6). *p<0.05 vs TG by Two-way ANOVA followed by Bonferroni multiple comparison test.

Supplementary Figure S8

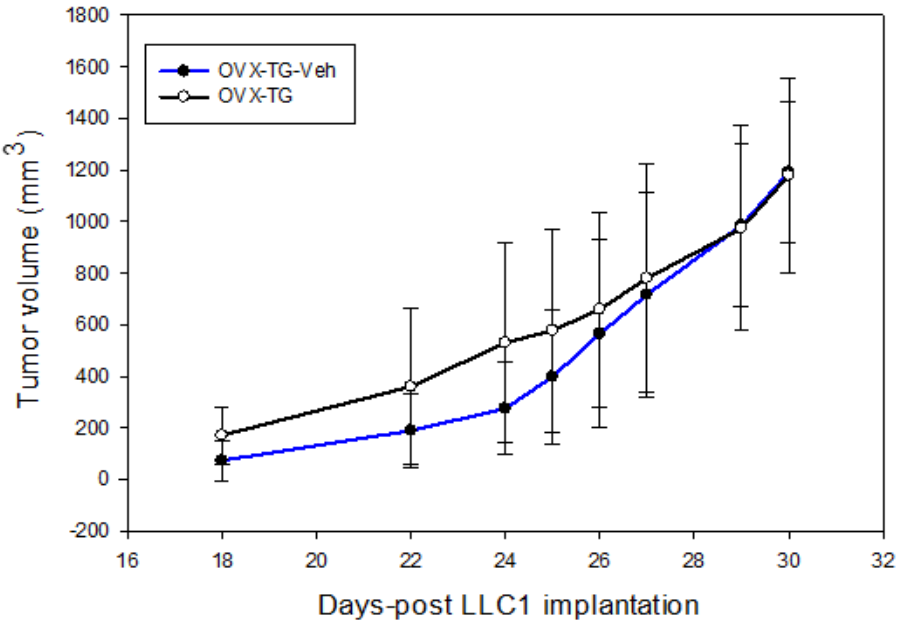

Fig. S8. Ovariectomized transgenic vehicle-treated or untreated mice display no significant difference in tumor volumes. Values represent arithmetic mean ± SD, (n=7). Two-way ANOVA followed by Bonferroni multiple comparison test was applied to demonstrate lack of significance.

Supplementary Figure S9

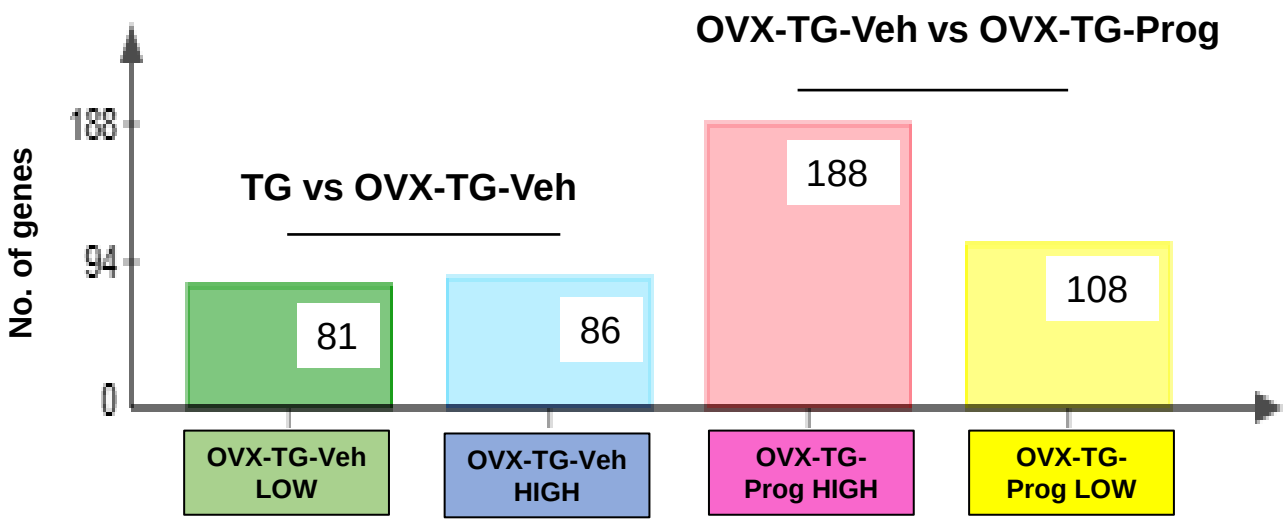

Fig. S9. Transcriptomics-based identification of differentially-expressed genes in LLC1 tumors excised from TG mice. Tumors were harvested at thirty days post-LLC1 tumor cell implantation, RNA-sequencing carried out and differentially-expressed genes identified. Comparisons between tumors isolated from TG mice vs ovariectomized-TG-vehicle treated (OVX-TG-Veh) mice, and from OVX-TG-Veh mice vs ovariectomized-TG-progesterone treated (OVX-TG-Prog) mice are shown. For OVX-TG-Veh, “LOW” and “HIGH” refer to comparisons with tumors from TG mice. For OVX-TG-Prog, “LOW” and “HIGH” refer to comparisons with tumors from OVX-TG-Veh mice.

Supplementary Figure S10

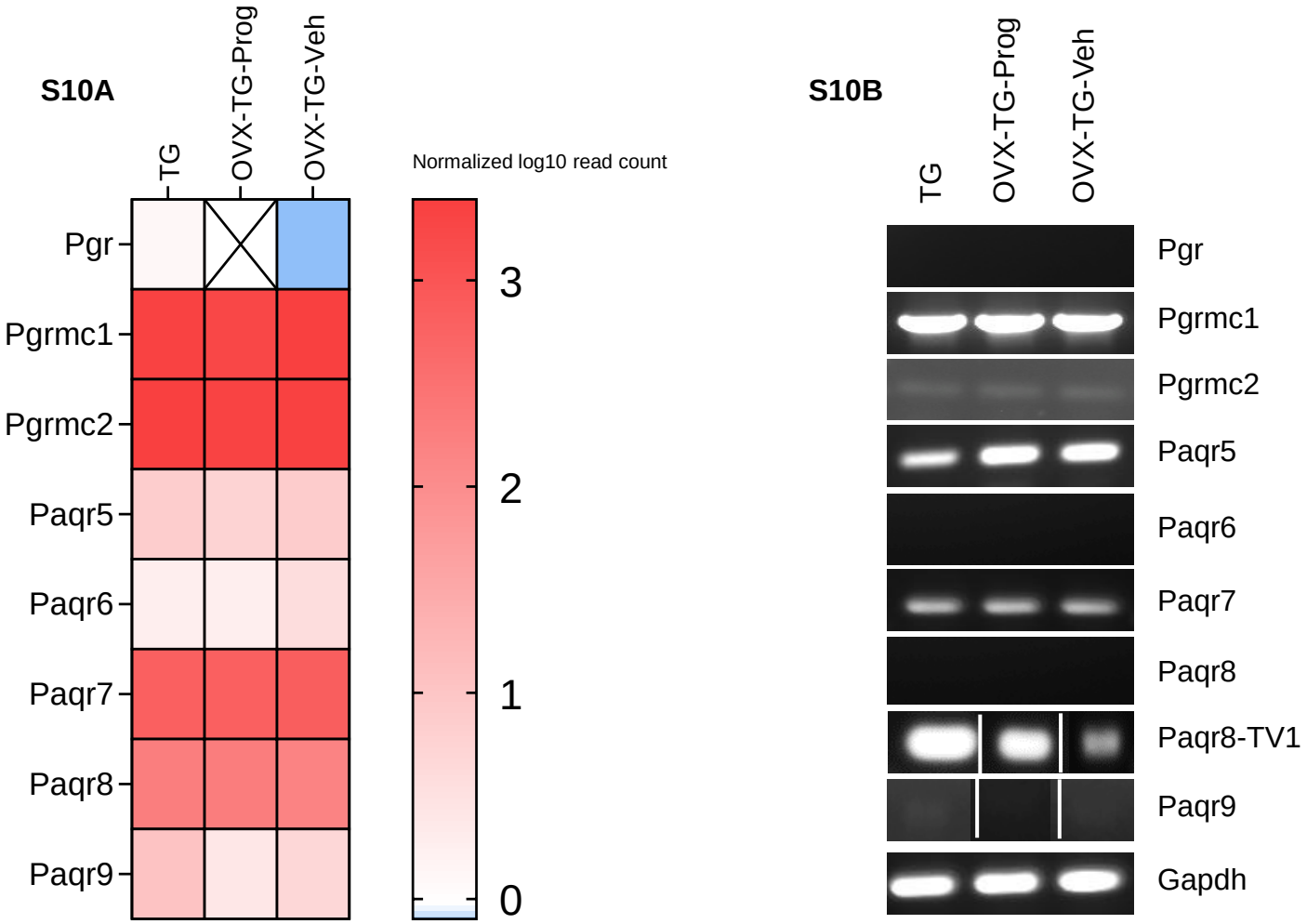

Fig. S10. LLC1 tumors do not express nuclear progesterone receptors but do express several non-nuclear progesterone receptors. (A) Heat map post-RNAseq analysis, displaying mRNA levels of nuclear and non-nuclear receptors in tumors derived from TG mice, OVX-TG-Prog mice and from OVX-TG-Veh mice. The cross denotes a value (log 10 of 0) that cannot be represented. (B) Validation of RNA-seq data by PCR. 1 μg of total RNA derived from TG mice, OVX-TG-Prog mice and from OVX-TG-Veh mice was converted to cDNA, and PCR was carried out. White lines indicate missing wells in the gel (raw data provided).

Supplementary Figure S11

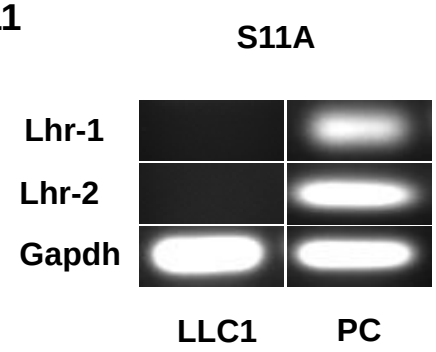

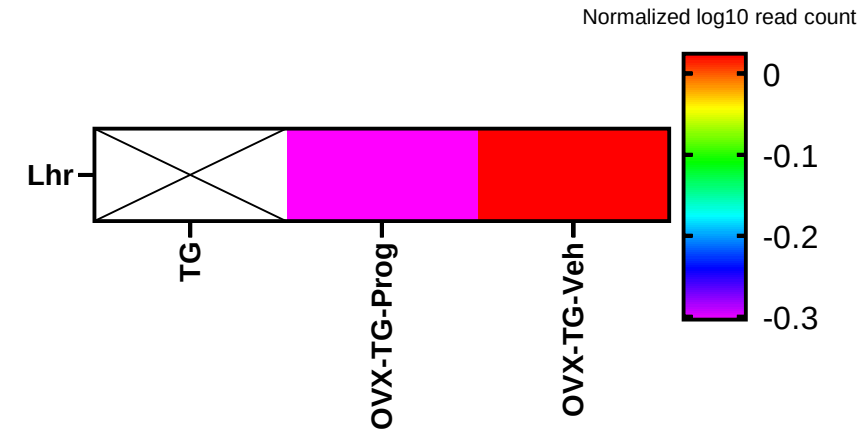

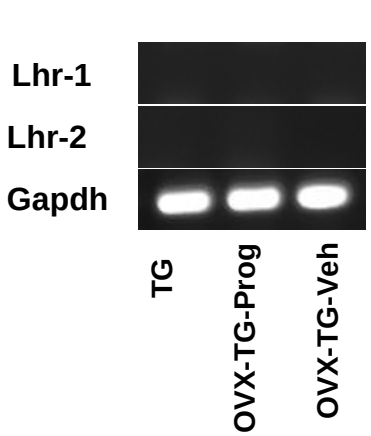

Fig. S11. LLC1 tumor cells in culture and excised LLC1 tumors do not express the conventional LH/hCG receptor. (A) 1 μg of total RNA isolated from LLC1 tumor cells in culture was converted to cDNA and PCR was carried out for two isoforms of the LH receptor (Lhr-1, Lhr-2). Murine ovaries was employed as a positive control (PC). Vertical gaps indicate missing wells in the gel (raw data provided). (B) Heat map post-RNAseq analysis, displaying mRNA levels of Lhr in tumors derived from TG mice, OVX-TG-Prog mice and from OVX-TG-Veh mice. The cross denotes a value (log 10 of 0) that cannot be represented. (C) 1 μg of total RNA isolated from tumors derived from TG mice, OVX-TG-Prog mice and from OVX-TG-Veh mice was converted to cDNA and PCR was carried out. S10C and S9B have same Gapdh controls since it corresponds to identical tumor samples (raw data provided).

Supplementary Figure S12

S12A

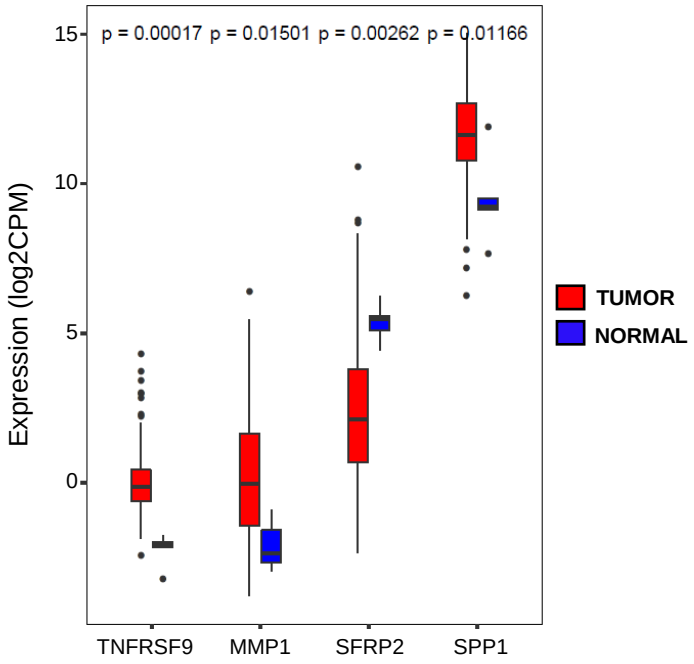

S12B

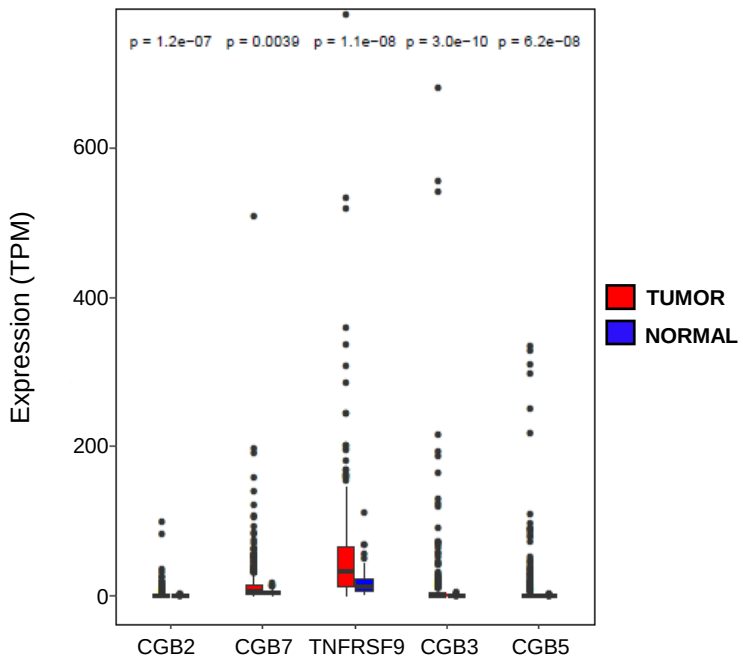

Fig. S12. Progesterone-influenced genes identified by RNA-seq in murine tumors display clinical relevance in humans. (A) Expression of the indicated genes in the GBM TCGA database. (n, tumor/normal=169/5). (B) Expression of the indicated genes in the LUAD TCGA database. (n, tumor/normal=517/59). In both cases, the Wilcoxon test was employed to assess significance.

Supplementary Figure S13

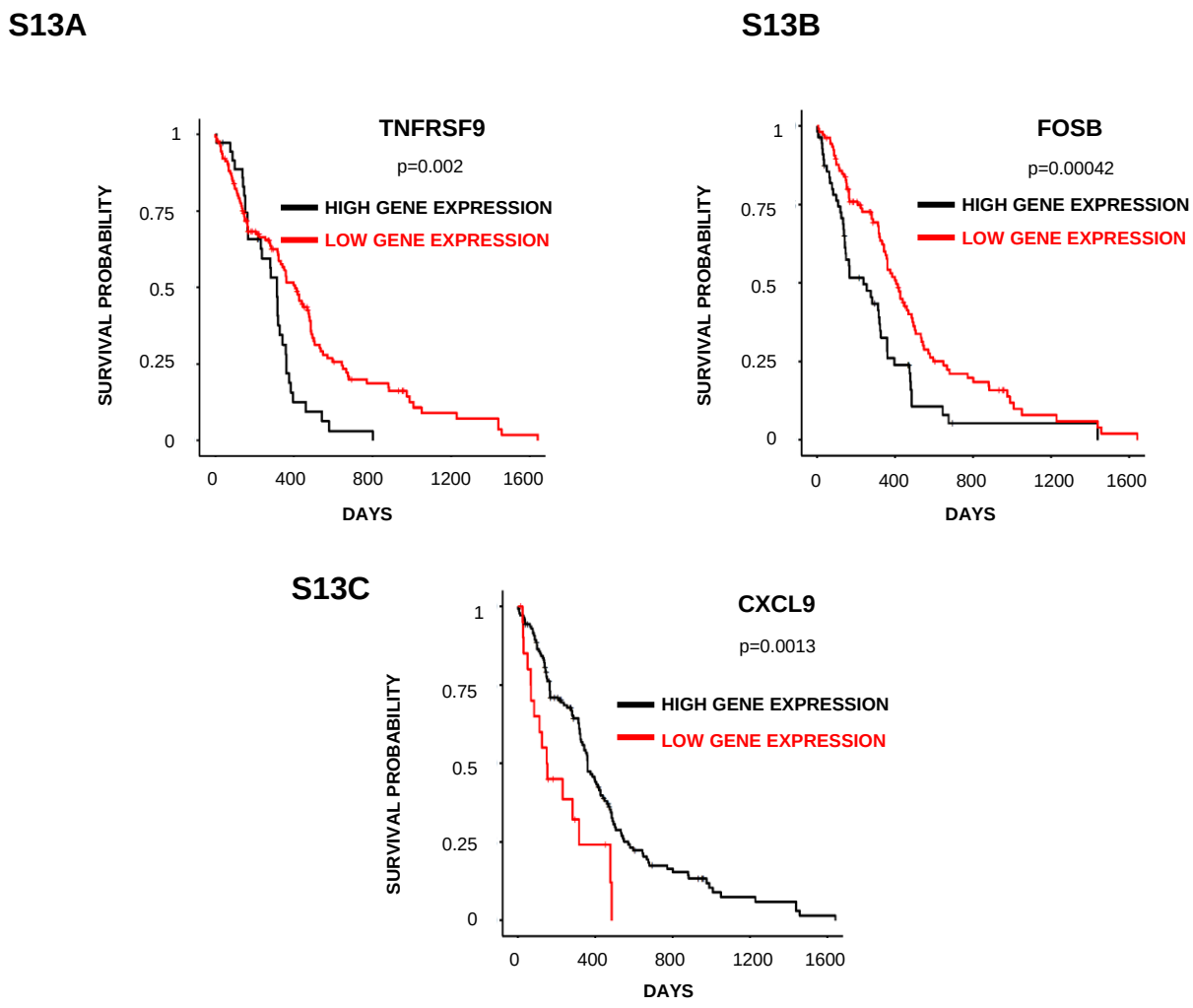

Fig. S13. Progesterone-influenced genes identified by RNA-seq in murine tumors display clinical relevance in humans. Survival analysis data derived from the GBM TCGA data base based on expression levels of the indicated genes in tumors. (A) TNFRSF9 (n, high/low=37/131); (B) FOSB (n, high/low=57/111); (C) CXCL9 (n, high/low=144/24). In all cases, the Logrank test was employed to determine significance, depicted in each panel.

Supplementary Figure S14

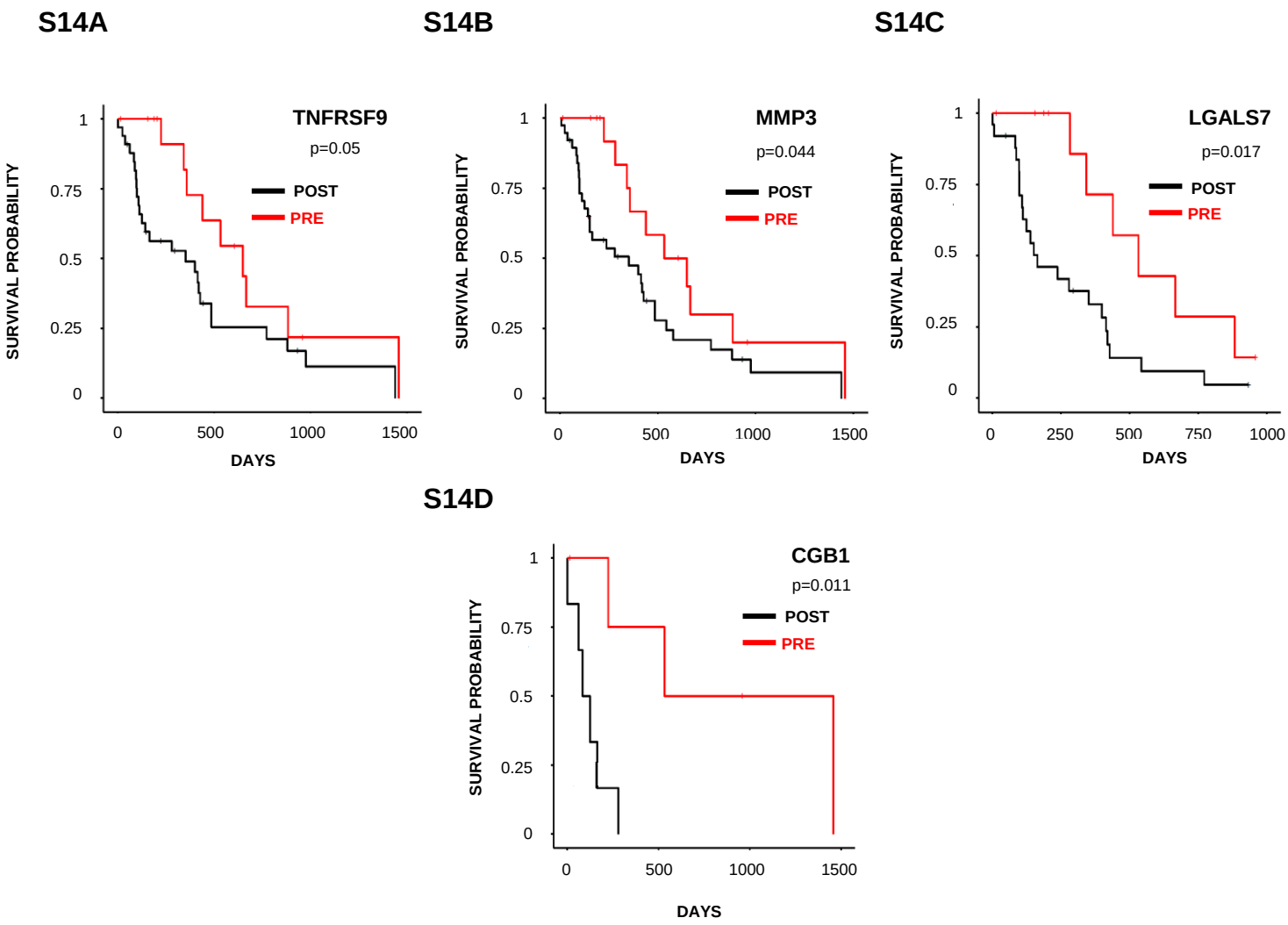

Fig. S14. Molecular profiling and TCGA analysis reveal the oncoprotective nature of pre-menopausal reproductive status. Survival analysis data derived from the TCGA-GBM data base based on low expression levels of the indicated genes in tumors. (A) TNFRSF9 (n, post/pre=34/15); (B) MMP3 (n, post/pre=39/16); (C) LGALS7 (n, post/pre=26/11); (D) CGB1 (n, post/pre=6/5). In all cases, the Logrank test was employed to determine significance, depicted in each panel. POST: Post-menopausal women; PRE: Pre-menopausal women.

Supplementary Figure S15

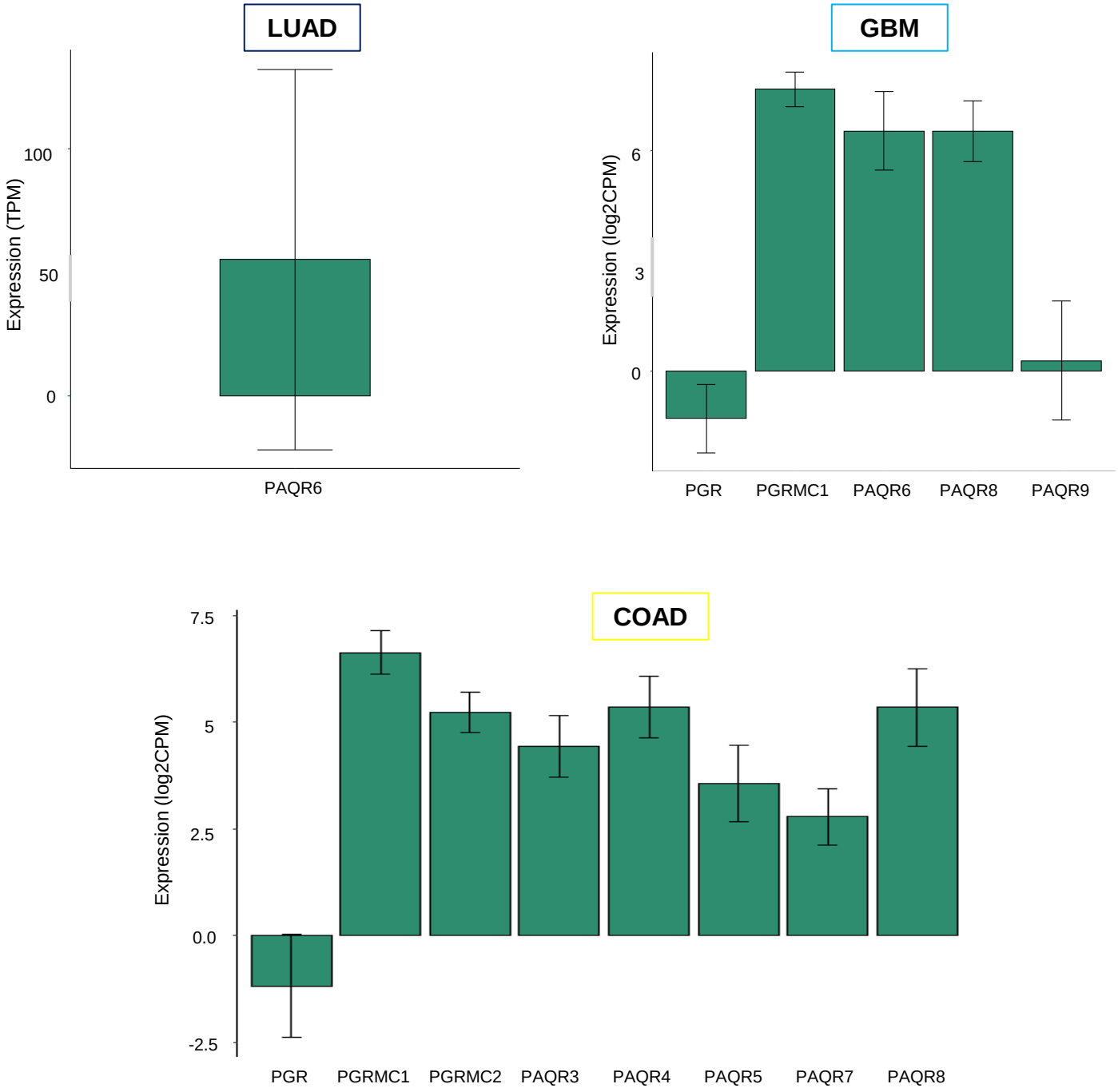

Fig. S15. Tumors in post-menopausal women express several non-nuclear progesterone receptors. Expression of the indicated receptors in LUAD (n=233), GBM (n=44), and COAD (n=164) in post-menopausal subjects. Values represent arithmetic mean expression ± SD.

Supplementary Table S1: Primer sequences of all genes included in this study

Gene (Murine)	Forward Primer	Reverse Primer	Tm	Amplicon Size (bp)
Pgr	CAATGGAAGGGCAGCATAACT	CTCTCGTTAGGAAGGCCCAC	65	217
Gapdh (Semiq-PCR control)	GGAGAGTGTTTCCTCGTCCC	ACTGTGCCGTTGAATTTGCC	66	202
Pgrmc1	GGGACTCTCAGTTCACTTTCAA	AGCACATACCTGTTCCTGCC	63	923
Pgrmc2	GGGCCGTGGTATGAATGTCT	GGTTTCCCCCTCATCGTGAA	67	209
Paqr5	CTATCCAGAGCTGCCTGTCC	CTACTCCATTGCTTCCCCAC	63	331
Paqr6	CCACCTGGTTCCCAGAGCTA	CCTCTTGGGTCTTCCGTCCT	66	691
Paqr7	GAAGGGTGAGGAGTTTGCAG	CTAGGGCATATCAGGGACCA	63	161
Paqr9	TTCTCAGCTTGCCACTCAGG	TCAGCCAAAGGAGCCTAACG	66	766
Paqr8	ACCCGTGACGCCCGTGAGAA	CTGATTTTGCAGGGTGACAAACTCCAT	73	460
Paqr8-TV1	GTCGGGGAGGCTCAGAAAGA	GGCTCAGTTAGACAACCTTTGTA	65	288
Fas	GTCCTGCCTCTGGTGCTTG	GGGTGCAGTTTGTTTCCACC	66	331
FasL	TGAAAAGCAAATAGCCAACCC	AAAAACGGCCTCTGTGAGGT	64	851
Bax	ATGGAGCTGCAGAGGATGAT	AGCCACCCTGGTCTTGGA	65	253
Bak1	CCTGGAACCCAACAGCATCT	TTACGGTCAGGATGGGGTCT	66	383
Mmp3	GGCGCAAATCTCTCAGGACT	AGCCCAGAACTGATTTCCTTT	64	N/A
Mmp12	GGTGGTACACTAGCCCATGC	AGGAAGAGGTTTGTGCCTTGA	64	N/A
Mmp1a	GCAAGGAGATGATGGCTGAA	CACACCTGGGCTTCTTCATAG	64	N/A
Mmp1b	ACCTTTGATCGATGTGATAGACCTT	CAGCCCATACTTTGCTGCCTTT	66	N/A
Hspa1a	ACGTGGGCTTTATCTTCCCTG	AACAAATCACATCAGCGGGG	66	N/A
Hspa1b	TGCACTGTACCAGGGGATTATG	AGGGAACTGGGCAGCTAGAC	65	N/A
Sprr1a	GCTCTTCTCTGAGTATTAGGACCA	GTTTTGGGGGCACAAGGTTC	65	N/A
Spp1	GCCAAGAGTGTGTTTGAACCT	AGAATCAGTCACTTTCACCGGG	64	N/A
Fos	CCTACTGTGTTCCTGGCAATAG	ACATTGACGCTGAAGGACTAC	61	N/A

Clu	CCAGGGAGTGAAGCACATAAA	CTCCAGAGCATCCTCTTTCTTC	64	N/A
Cxcl9	TCGGACTTCACTCCAACACA	CCTTATCACTAGGGTTCCTCGAA	64	N/A
Adm	TACGGGACTCGCTGATGAGA	CTTCGCTCTGATTGCTGGCT	66	N/A
Timp3	TTCTGCAACTCCGACATCGT	AGCCTCGGTACATCTTCATCT	64	N/A
Tnfrsf9	ATTCTTCTTCACCTTTGGTGTCCT	CTTCTCACAGCCCACTAGCAG	64	N/A
Actin (RT-PCR control)	CTCTGGCTCCTAGCACCATGAAGA	GTAAAACGCAGCTCAGTAACAGTCCG	66	N/A
Lhr (Isoform 1)	CGAGACGCTTTATTCTGCCATC	CACAGGGATTGAAAGCATCTGG	66	122
Lhr (Isoform 2)	GCTGACCTACCCTAGCCACT	CAGAGTGATGAAGCGTCTCGT	63	143
Beta-hCG	CGCGCCCTCGTCGTGTC	AAGCGGGGGTCATCACAGGTC	55	830
Actin (Genomic PCR control)	TCCTATGGGAGAACGGCAGA	TCCTTTGTCCCCTGAGCTTG	61	676

Supplementary Table S2: Includes information of all reagents and other resources included in this study

Item	Source	Catalog number
Caspase-8	Cell Signaling Technology	4790
Cleaved Caspase-8	Cell Signaling Technology	8592
Caspase-9	Cell Signaling Technology	9508
Caspase-3	Cell Signaling Technology	9662
Caspase-7	Cell Signaling Technology	9492
Phospho-p38	Cell Signaling Technology	9211
p38	Cell Signaling Technology	9212
Phospho-JNK	Cell Signaling Technology	9255
JNK	Cell Signaling Technology	9252
Phospho-ERK1/2	Cell Signaling Technology	4370
ERK1/2	Cell Signaling Technology	4695
MMP12	Invitrogen	PA5-86640
FOS	Invitrogen	MA5-36080
ADM	Invitrogen	PA5-36524
HSPA1A	Invitrogen	PA5-34772
CXCL9	Invitrogen	PA5-81371
MMP3	Invitrogen	PA527936
Peroxidase conjugated AffiniPure goat anti-mouse IgG+IgM (H+L)	Jackson Immuno Research	115-035-068
Goat anti-mouse IgG, human ads-HRP	Southern Biotech	1030-05
Peroxidase AffiniPure goat anti-rabbit IgG (H+L)	Jackson Immuno Research	111-035-144
Goat anti-rabbit IgG H&L-HRP	Abcam	ab6721
GAPDH	Cell Signaling Technology	2118
MTT	Invitrogen	M6494

^{3}H-Thymidine	American Radiolabeled Chemicals	ART0178B
Annexin-V-PE	BD Biosciences	556421
DMEM High Glucose	Gibco	12100046
Antibiotic-antimycotic (100X)	Gibco	15240062
DMSO (For cell culture)	Sigma-Aldrich	D2438
Fetal bovine serum, qualified, Brazil	Gibco	10270106
Fetal bovine serum, EU Approved, charcoal treated	Himedia	RM10416
StemPro™ Accutase™ cell dissociation reagent	Gibco	A1110501
Trypsin-EDTA (0.25%), phenol red	Gibco	25200056
Mifepristone	Sigma-Aldrich	M8046
Progesterone	Sigma-Aldrich	P8783
Beta-Estradiol	Sigma-Aldrich	E2758
Cholesterol	Sigma-Aldrich	C3045
Ethanol	Merck	64-17-5
hCG	Sigma-Aldrich	C0434
Native human hCG beta protein	Abcam	ab126653
Z-VAD-FMK	Sigma-Aldrich	627610
Tamoxifen	Enzo	ALX-550-095-G001
Inhibitor JNK II	Calbiochem	420119
Inhibitor ERK_PD98059	Calbiochem	513000
Inhibitor p38_SB203580	Calbiochem	559389

RT-PCR FG-POWER SYBR GREEN PCR MASTER MIX	Thermo Fisher Scientific	4367659
3B DNA Polymerase (5U/ul) with 10X reaction buffer (with 20 mM $MgCl_2$)	3bblackbio (Biotools)	3B010
DMSO (for analytical assays)	Amresco	0231
Propidium iodide	Invitrogen	P3566
Annexin-V-FITC	BD Biosciences	556419
DMSO (Molecular biology grade)	Sigma-Aldrich	D9170
TRIzol	Thermo Fisher Scientific	15596018
Chloroform	Sigma-Aldrich	C2432
2-Propanol	Sigma-Aldrich	I9516
Nuclease-free water	Promega	P1197
3-Isobutyl-1-methylxanthine (IBMX)	Calbiochem	410957
Ro-20-1724	Calbiochem	557502
Annexin-V binding buffer	BD Biosciences	51-66121E
DPX	Sigma-Aldrich	06522
Protease inhibitor	Thermo Fisher Scientific	A32955
Phosphatase inhibitor	Thermo Fisher Scientific	A32957
Nitrocellulose membrane	Bio-rad	1620112
Difco skimmed milk	BD Biosciences	232100
BSA	Merck	A7906
ECL	Bio-rad	1705061
X-ray film	Carestream	6568307
Proteinase K	Qiagen	1017738

Iodogen	Thermo Fisher Scientific	28600
3 color pre-stained protein ladder	Puregene (representative image in the raw data)	PG-PMT2922
100bp DNA ladder RTU	Gene Direx	DM001-R500
RNAlater	Qiagen	1018087
Commercial kits		
cAMP glo assay	Promega	V1501
CellTiter Glo® luminescent cell viability assay (ATP assay)	Promega	G9242
Mouse prolactin ELISA kit	R and D systems	DY1445
Verso cDNA synthesis kit	Thermo Fisher Scientific	AB1453A
Micro BCA protein assay kit	Thermo Fisher Scientific	23235
EnVision Flex+, mouse, high pH	Dako	K8002
Cell lines		
LLC1	ATCC	CRL-1642
A549	ATCC	CCL-185
Software and algorithms		
Sigma Plot	Version 12.5	
Graphpad Prism	Version 8	
ImageJ	https://imagej.nih.gov/ij/download.html	
DAVID	https://david.ncifcrf.gov/	
Flow Jo	Version 10.8.1	
"Quest Graph™ Four parameter logistic (4PL) curve calculator." *AAT Bioquest, Inc*, 13 Nov. 2021.	https://www.aatbio.com/tools/four-parameter-logistic-4pl-curve-regression-online-calculator.	AAT Bioquest
TCGA	Relevant links mentioned in methods	

Primer-Blast	https://www.ncbi.nlm.nih.gov/tools/primer-blast/	
IDT OligoAnalyzer Tool	https://www.idtdna.com/pages/tools/oligoanalyzer	
jvenn	http://jvenn.toulouse.inra.fr/app/example.html	
FastQC	http://www.bioinformatics.babraham.ac.uk/projects/fastqc/	
Trimgalore	https://github.com/FelixKrueger/TrimGalore	
Other Items		
Thermo Scientific™ Nunc™ F96 microWell™ white polystyrene plate	Thermo Scientific	136101
All other common chemicals	Sigma/Merck	N/A
Cautery system	Gemini	GEM-5917
Autoclip 9mm applier	Stoelting	59043
Autoclip remover	Stoelting	59046
Autoclips	Stoelting	59047

Supplementary Table S3: Summary of immunohistochemical analysis of data presented in Fig. 5G.

GENE	TG	OVX-TG-Veh	OVX-TG-Prog
Mmp3	Moderate expression in the cytoplasm of few tumor cells.	Higher expression in extracellular matrix as compared to the cytoplasm of most tumor cells	Low expression in the cytoplasm of few tumor cells.
Mmp12	Moderate expression in the cytoplasm of few tumor cells.	Higher expression in extracellular matrix as compared to the cytoplasm of most tumor cells	Low expression in the cytoplasm of few tumor cells and in the extracellular matrix
Adm	Moderate expression in the cytoplasm of few tumor cells.	Moderate to high expression in the cytoplasm of most tumor cells.	Low expression in the cytoplasm of few tumor cells
Hspa1a	High expression in the cytoplasm of many tumor cells.	Moderate expression in the cytoplasm of tumor cells.	Low expression in the cytoplasm of few tumor cells
Fos	High expression in the cytoplasm of many tumor cells.	High expression in the cytoplasm of many tumor cells.	Moderate expression in the cytoplasm of few tumor cells
Cxcl9	No expression was observed in tumor cells	Moderate expression in the cytoplasm of few tumor cells.	Moderate expression in the cytoplasm of few tumor cells.